

Molecular cloud chemistry and the importance of dielectronic recombination

P. Bryans,¹ H. Kreckel,¹ E. Roueff,² V. Wakelam³ and D. W. Savin,¹

ABSTRACT

Dielectronic recombination (DR) of singly charged ions is a reaction pathway that is commonly neglected in chemical models of molecular clouds. In this study we include state-of-the-art DR data for He^+ , C^+ , N^+ , O^+ , Na^+ , and Mg^+ in chemical models used to simulate dense molecular clouds, protostars, and diffuse molecular clouds. We also update the radiative recombination (RR) rate coefficients for H^+ , He^+ , C^+ , N^+ , O^+ , Na^+ , and Mg^+ to the current state-of-the-art values. The new RR data has little effect on the models. However, the inclusion of DR results in significant differences in gas-grain models of dense, cold molecular clouds for the evolution of a number of surface and gas-phase species. We find differences of a factor of 2 in the abundance for 74 of the 655 species at times of 10^4 – 10^6 years in this model when we include DR. Of these 74 species, 16 have at least a factor of 10 difference in abundance. We find the largest differences for species formed on the surface of dust grains. These differences are due primarily to the addition of C^+ DR, which increases the neutral C abundance, thereby enhancing the accretion of C onto dust. These results may be important for the warm-up phase of molecular clouds when surface species are desorbed into the gas phase. We also note that no reliable state-of-the-art RR or DR data exist for Si^+ , P^+ , S^+ , Cl^+ , and Fe^+ . Modern calculations for these ions are needed to better constrain molecular cloud models.

Subject headings: astrochemistry — atomic data — atomic processes — ISM: atoms — dust, extinction — ISM: molecules

¹Columbia Astrophysics Laboratory, Columbia University, 550 West 120th St, MC 5247, New York, NY 10027-6601

²LUTH and UMR 8102 du CNRS, Observatoire de Paris, Section de Meudon, Paris, France

³Université Bordeaux, Laboratoire d'Astrophysique de Bordeaux, CNRS/INSU, UMR 5804, BP89 33271 Floirac Cedex, France

1. Introduction

Investigating the physics and chemistry of molecular clouds (also known as quiescent cores) is crucial if one is to understand the processes that ultimately lead to star formation. Such studies are also important in the field of astrobiology since these clouds are the birthplace of the first organic molecules.

Chemical models used to describe the evolution of molecular clouds typically include hundreds of species. At molecular cloud temperatures ($\lesssim 100$ K) these atoms and molecules are either neutral or singly ionized. The abundances of these species are, in turn, governed by thousands of reactions that are highly non-linear. These derived abundances are sensitive to the accuracy of the rate coefficients involved. The implication of uncertainties in the rate coefficients used in chemical models has been investigated by Roueff et al. (1996), Vasyunin et al. (2004, 2008), Wakelam et al. (2005, 2006), and others. However, these studies cannot account for reaction processes that are not included in the models in the first place.

To the best of our knowledge, the only recombination process of free electrons with atomic ions included in any molecular cloud simulation is radiative recombination (RR). Recent calculations by Badnell (2006)¹ have improved the accuracy of the rate coefficients of these reactions for a number of ions. The alternative pathway of dielectronic recombination (DR) has previously not been included in molecular cloud models. This is largely due to the bulk of published DR calculations and experiments being valid only for plasmas of higher temperature. Recently, however, theoretical calculations by Badnell et al. (2003)² have probed DR at the low temperature regimes of molecular clouds. At these temperatures, the DR rate coefficient can be a factor of 5 or more greater than the RR rate coefficient for certain systems.

In the present paper, we both update the RR data and include DR for the relevant singly charged atomic ions. We do this for several molecular cloud models under a variety of initial conditions. We use Nahoon (Wakelam et al. 2004) to simulate dense clouds and protostars, the OSU gas-grain code (Hasegawa et al. 1992; Garrod & Herbst 2006) to simulate dense clouds, and the Meudon Photodissociation Region (PDR) code (le Petit et al. 2002, 2006) to simulate both diffuse and dense PDRs. We compare the species abundances with those calculated with and without DR included in order to show the effects on the models. The remainder of the paper is organized as follows: In Sec. 2 we review the recent developments

¹<http://amdpp.phys.strath.ac.uk/tamoc/RR/>

²<http://amdpp.phys.strath.ac.uk/tamoc/DR/>

in our understanding RR and DR. Section 3 outlines the chemical models we use to simulate dense clouds, diffuse clouds, and protostars. In Sec. 4 we present the results of including DR in these chemical models. Concluding remarks are given in Sec. 5.

2. Recombination data

2.1. Radiative Recombination

Radiative recombination (RR) is a one-step recombination process that occurs when a free electron is captured by an ion. Energy and momentum are conserved in the process by the simultaneous emission of a photon. At the low temperatures typical of molecular clouds, RR is the dominant ion-electron recombination process for most ions. Until now, the molecular cloud codes that we use in the present work (see Sec. 3) have used RR rate coefficients from the UMIST database³ (Woodall et al. 2007). For the most part it is unclear where the RR data in the UMIST database stem from as there is often no reference given; this is the case for the rate coefficients of H^+ , He^+ , Na^+ , Mg^+ , Si^+ , P^+ , S^+ , Cl^+ , and Fe^+ . There is no RR data for F^+ . For C^+ and N^+ the rate coefficients are those of Nahar & Pradhan (1997) and for O^+ the rate coefficient is from Nahar & Pradhan (1999). The data of Nahar & Pradhan are actually unified RR+DR calculations using LS-coupling. As a result, they have no DR component at the low temperatures of molecular clouds since they do not account for fine structure transitions of the ground term (see Sec. 2.2).

In recent years there have been attempts to better understand the RR process using state-of-the-art computational techniques. Badnell (2006) has calculated RR rate coefficients for all elements from H through Zn for bare through Mg-like isoelectronic sequences. We have implemented these calculations for the ions included in the chemical networks of the models considered here, namely H^+ , He^+ , C^+ , N^+ , O^+ , Na^+ , and Mg^+ . For the ions that Badnell (2006) has not calculated—namely Si^+ , S^+ , Cl^+ , and Fe^+ —we have used the rate coefficients recommended by Mazzotta et al. (1998). These come from Aldrovandi & Péquignot (1973) for Si^+ and S^+ ; an extrapolation of the S-like sequence is used to estimate the Cl^+ rate coefficient; and the rate coefficient from Schull & van Steenberg (1982; refitted with the Verner & Ferland 1996 formula) is used for Fe^+ .

At molecular cloud temperatures, the largest difference found between the RR rate coefficients of the UMIST dataset and the Badnell (2006) RR data is for Mg^+ , as is shown in Fig. 1. At a temperature of 10 K, typical of a cold molecular cloud, the UMIST rate

³<http://www.udfa.net/>

coefficient is 60% larger than that of Badnell.

2.2. Dielectronic recombination

Dielectronic recombination (DR) is a two-step recombination process that begins when a free electron collisionally excites a core electron of an ion and is simultaneously captured. The core electron excitation can be labeled $nl_j \rightarrow n'l'_{j'}$, where n is the principal quantum number, l the orbital angular momentum, and j the total angular momentum. The energy of this intermediate system lies in the continuum and the complex may autoionize. The DR process is complete when the system emits a photon, reducing the total energy of the recombined system to below its ionization threshold. Conservation of energy requires that for DR to go forward

$$E_k = \Delta E - E_b. \quad (1)$$

Here E_k is the kinetic energy of the incident electron, ΔE the excitation energy of the initially bound electron in the presence of the captured electron, and E_b the binding energy released when the incident electron is captured onto the excited ion. Because ΔE and E_b are quantized, DR is a resonant process occurring for a given channel at energies $E_k < \Delta E$.

For a molecular cloud of temperature T_{cloud} , the important DR channels are those where $\Delta E \sim k_B T_{\text{cloud}} \lesssim 0.01$ eV. Thus, from atomic energy structure considerations alone, it is clear that fine structure excitations of the ground term are important in molecular clouds. Until recently, the preponderance of DR data have been calculated using LS-coupling. However, this coupling scheme does not include these low-energy resonances. Recent state-of-the-art calculations by Badnell et al. (2003), using intermediate coupling, have accounted for these fine structure channels, calculating DR rate coefficients for H- through Mg-like ions of all elements from He through Zn.

For the singly-ionized ions of interest in molecular clouds— H^+ , He^+ , C^+ , N^+ , O^+ , F^+ , Na^+ , Mg^+ , Si^+ , P^+ , S^+ , Cl^+ , and Fe^+ —one would expect a significant low-temperature DR contribution for C^+ , N^+ , F^+ , Si^+ , P^+ , Cl^+ and Fe^+ due to their fine structure splitting of the ground term. The other ions either do not undergo DR (i.e., H^+) or have no such fine structure splitting. Of these five ions with fine structure splitting, Badnell et al. (2003) has calculated DR only for C^+ , N^+ , and F^+ . Figs. 2 and 3 show a comparison of the DR and RR rate coefficients for C^+ and N^+ , respectively. At temperatures $\lesssim 100$ K, typical of molecular clouds, the DR component dominates the electron-ion recombination rate coefficient highlighting the importance of including this recombination process. For the present work we have implemented the DR rate coefficients of Badnell et al. (2003) for He^+ , C^+ , N^+ , O^+ , F^+ , Na^+ , and Mg^+ . No such non-LS coupling calculations exist for Si^+ , P^+ , Cl^+ and Fe^+ .

3. Models

3.1. Nahoon

The Nahoon code (Wakelam et al. 2004) is a pseudo-time-dependent chemical model that computes the chemical evolution of gas-phase species for a fixed gas temperature and density. It is suited for modeling dense molecular clouds and protostars. The model includes 452 species with initial conditions being atomic (neutral and singly charged) He, C, N, O, F, Na, Mg, Si, P, S, Cl, and Fe plus molecular hydrogen. Dust grains are included in the model but are not fully treated; ions are allowed to neutralize by charge exchange with negative grains but accretion of species onto grains is not included, and thus no grain surface chemistry is possible. The code computes the evolution of the abundance of each species as governed by the 4423 included reactions between species. The reaction rate coefficients come from the osu.2005⁴ chemical network (Smith et al. 2004). The RR rate coefficients in this network are those from the UMIST database (see discussion in Sec. 2.1). We have replaced these RR rate coefficients with those of Badnell (2006) for H^+ , He^+ , C^+ , N^+ , O^+ , Na^+ , and Mg^+ . We have also added the DR reactions for He^+ , C^+ , N^+ , O^+ , Na^+ , and Mg^+ using the rate coefficients of Badnell et al. (2003). For the other ions that have not been calculated by Badnell et al. (2003) or Badnell (2006)— Si^+ , S^+ , Cl^+ , and Fe^+ —we have used the RR and DR rate coefficients of Mazzotta et al. (1998). While the elements F and P are present in Nahoon, recombination of F^+ and P^+ are not included. We have chosen not to introduce these processes and instead concentrate on the effect of the updated RR and DR rate coefficients for those reactions that are already present.

With these new reactions included, we have used Nahoon to simulate the evolution of dense cold clouds and protostars. A dense cold cloud is simulated by assuming a temperature of 10 K, an initial H_2 density of 10^4 cm^{-3} , a visual extinction of 10 so that the photochemistry driven by external UV photons does not occur, and a fixed cosmic-ray ionization rate of $1.3 \times 10^{-17} \text{ s}^{-1}$. These dense cloud conditions are given in Table 1. We use the low-metal elemental abundances of Graedel et al. (1982) as our initial conditions. These are also given in Table 1. For a protostar, we take our initial gas-phase chemical composition as that computed by Nahoon for the above dense cloud conditions at 10^5 years. Additionally, we increased the temperature to 100 K, the initial H_2 density to 10^7 cm^{-3} , and set the abundances of H_2O , H_2CO , CH_4O , and CH_4 as given in Table 1. This is required because Nahoon does not include the surface chemistry that is needed to form these species, so we artificially increase their abundance in the gas phase to simulate protostar conditions. Results for both dense

⁴http://www.physics.ohio-state.edu/~eric/research_files/osu.2005

clouds and protostars are presented in Sec. 4.

3.2. OSU gas-grain code

The OSU gas-grain code (Hasegawa et al. 1992; Garrod & Herbst 2006) is similar to Nahoon in that it follows the evolution of the species abundances as a function of time for a fixed cloud temperature and density. Like Nahoon, it is used to simulate the conditions of dense molecular clouds. However, unlike Nahoon, the OSU gas-grain code includes surface chemistry in addition to gas-phase chemistry. This allows for time-dependent accretion onto grain surfaces as well as thermal and cosmic ray-induced evaporation from the surfaces. The code assumes a sticking coefficient of unity for neutral species that strike grains. It is unclear whether charged species can also accrete onto grains (Watson 1976). It is assumed here that they do not, with the energy released on neutralization resulting in the species desorbing from the grain surface. This model also includes the new non-thermal evaporation mechanism of Garrod et al. (2007). This process assumes that the energy released by exothermic surface reactions partially evaporate the products.

Species can react on the grain surfaces to form molecules more efficiently than is possible solely in the gas phase. This surface chemistry is an important contributor to the species present in the warm-up phase of hot molecular cores (Garrod & Herbst 2006). Species that form on the grains at earlier times are injected into the gas phase when the dust is heated by a nearby protostar.

The OSU code uses the osu.2005 chemical network, although there is no F present in the OSU gas-grain code, unlike in Nahoon. With the addition of the surface species to the network used with Nahoon, there are 655 species and 6309 reactions. We added the new RR and DR rate coefficients in the same way as was done in Nahoon (see Sec. 3.1). With these changes to the chemical network, we have run the OSU code with the same initial conditions as used in Sec. 3.1 when simulating a dense cold cloud (see Table 1). We present our results in Sec. 4.

3.3. PDR code

In order to simulate a molecular cloud with a significant impinging radiation field, we use the PDR code of the Meudon group (le Petit et al. 2002, 2006)⁵. This code is used to

⁵<http://aristote.obspm.fr/MIS/pdr/pdr1.html>

simulate clouds with no rapidly evolving processes occurring. The cloud is treated in steady state as an infinite slab of gas and dust irradiated by an ultraviolet radiation field impinging on both sides of the cloud. While dust is included in the model, there is no surface chemistry other than allowing for the formation of H_2 which cannot be produced rapidly enough in the gas phase.

Using a standard chemistry file with 120 species we have added the new RR and DR data to the PDR code. The elemental abundances are given in Table 1. We have run the model with physical conditions that simulate a diffuse PDR and, separately, a dense PDR. For diffuse conditions, we set the H_2 density to 25 cm^{-3} , the temperature to 20 K, and the cosmic ray ionization rate of $5 \times 10^{-17} \text{ s}^{-1}$. The radiation field is 1 Draine at the edges of the cloud. For a dense PDR, we simulate the Horsehead nebula (Pety et al. 2005) with an H_2 density of $5 \times 10^4 \text{ cm}^{-3}$, a temperature of 90 K, and a cosmic ray ionization rate of $5 \times 10^{-17} \text{ s}^{-1}$. For this case the radiation field is 100 Draine at the edge of the cloud. The species abundances are calculated as a function of depth into the cloud. Results are presented in Sec. 4.

4. Results

For each of the models described in Sec. 3 we have run the simulation with the original chemical network without any additions, with just the new RR, and again with the new RR and DR rate coefficients included. When running the models with only the new RR data included we find no differences greater than a factor of 2 for any of the models. Only for the OSU gas-grain code do we find abundance differences of greater than 50%. These are found for gas-phase Fe, surface FeH, and surface MgH_2 , resulting from the change in the Mg^+ and Fe^+ RR rate coefficients. The more significant results reported in the remainder of this section can thus be attributed primarily to the effect of DR on the models.

Simulations of a dense, cold molecular cloud of low metallicity were run with the OSU gas-grain code, which computes both gas-phase and surface chemistry. We find that the introduction of DR results in significant differences in certain species evolution. To identify those differences that are most important in the cloud chemistry we consider differences only at times when species have an abundance (either before or after the inclusion of DR) of at least 10^{-12} with respect to the total H nuclei density. This represents those species that are most likely to be detectable. Secondly, we only consider abundances at times of 10^4 – 10^6 years in the model evolution as it is during this period in the evolution of the model that observed molecular cloud conditions are best represented. With these criteria, we find 100 species to have a difference in abundance of at least 50% on including DR. We list in Table 2 the 74

species for which we find at least a factor of 2 difference in abundance. Of these 74 species 48 are attached to the surface of dust grains and 26 are found in the gas phase. The effect of the new DR rate coefficients on species abundances is over 2 orders of magnitude for 16 species. The greatest effect is found for surface O_3 , with a 3 orders of magnitude difference in abundance found. In Figs. 4, 5, and 6 we show the evolution of the abundance of surface C, surface CH_3OH , and surface O_3 , respectively.

We have run the gas-grain model a number of times, including DR for only a single selected ion in each run, and repeated this for every ion. This allows us to determine which ion has the largest effect on the differences we have found. These results indicate that the abundance differences listed in Table 2 are primarily due to the introduction of the C^+ DR. When the C^+ DR rate coefficient is not included in the model we find no differences in abundance greater than a factor of 2. The inclusion of DR increases the C^+ recombination rate, neutralizing C earlier in the model evolution. The model allows neutral species to accrete onto grains but not charged species. Thus, with an increased abundance of neutral C, the surface chemistry is enriched and results in the abundance differences that we observe.

Despite the large increase in the electron-ion recombination rate coefficient for N^+ (Fig. 3), the comparatively small effect of the inclusion of N^+ DR can be explained by considering the ionization balance of N in the simulation. Initially (see Table 1) all N in the model is in the neutral charge state, so recombination of N^+ with a free electron is not possible. As the model evolves, some N^+ is formed but neutral N remains many orders of magnitude greater in abundance.

In contrast, atomic C, due to its lower first ionization potential, is initially all singly ionized by UV radiation shortward of the 13.6 eV ionization potential of H but above the 11.3 eV ionization potential of C (again see Table 1). Thus, recombination of C^+ is important from the very start of the model evolution and the inclusion of DR greatly increases the electron-ion recombination rate. The increase in the C recombination rate also results in a change in the ionization fraction of the gas as can be seen in the abundance evolution of the sum of all negatively charged species. To show this we plot the free electron abundance in Fig. 7. The abundance of all other negatively charged species are negligible in comparison.

To investigate the importance of the surface chemistry on our results, we have run the gas-grain model with no accretion of species onto dust grains allowed. We have compared results with and without DR included. With the surface chemistry excluded, we find differences in abundance of 50% for 32 species but factor of 2 increases for only 5 species— CH_3CN , CH_3CO^+ , HC_2NC , C_3H_3^+ , and HC_3N . These 5 gas-phase molecules had among the smallest changes of the 74 species we identified as having a factor of 2 difference when the surface chemistry was included. Of the 74 species listed in Table 2, 48 are surface species which are

unable to form when we do not include the surface chemistry. However, there are also 26 gas-phase species in Table 2. Only the 5 gas-phase species identified above have differences of a factor of 2 when the surface chemistry is excluded. Of the 21 other gas-phase species in Table 2, 11 have no formation routes without the surface chemistry included. The other 10, whose abundances are greatly enhanced by formation routes on grain surfaces, have changes of less than 50% in a purely gas-phase model. Thus, the majority, and indeed the largest, abundance differences seen when including DR in the OSU gas-grain model are found for species influenced by surface reactions.

Not surprisingly then, we do not find significant abundance differences when running the dense cloud simulation using Nahoon, which does not include grain surface chemistry. All species in Nahoon are in the gas phase. The introduction of the DR data resulted in 20 species having an abundance difference of 50% and only 2 species, OCS and $\text{C}_2\text{H}_3\text{N}$, having abundance increases of greater than a factor of 2. When running the protostar simulation using Nahoon we again find few significant differences when DR is included; 21 species have an abundance difference of 50% or more. The only species with greater than a factor of 2 difference are C_2S , HCN, HNC, $\text{C}_2\text{H}_3\text{N}$, HCOOCH_3 , CH_3OCH_3 , H_2CN^+ , and $\text{CH}_3\text{OCH}_4^+$, all of which are increased in abundance with DR relative to without.

Simulations of diffuse and dense PDRs were carried out using the Meudon PDR code, allowing us to probe the effect of DR in a molecular cloud with a radiation field present. On introducing the new DR rate coefficients there is a large increase in the total recombination rate of C^+ and we see a significant effect on the abundance of neutral carbon as a result. This is the case for both diffuse and dense PDRs. The column density of C is shown in Figs. 8 and 9 for diffuse and dense regions, respectively, as a function of visual extinction (i.e., depth into the cloud). However, we find no significant abundance differences for any other species in the diffuse case. For a dense PDR, there are only 5 other species that show an abundance difference greater than 50%— SO_2 , O_2H^+ , HSO_2^+ , HOCS^+ , and C_4 . These species all increase in abundance with the introduction of DR but the increases are all less than a factor of 2.

5. Conclusions

This work has investigated the importance of new RR and DR rate coefficients in molecular cloud models. We have updated the RR rate coefficients of H^+ , He^+ , C^+ , N^+ , O^+ , Na^+ , and Mg^+ to the current state-of-the-art in 3 different molecular cloud chemical models. We have run these models under different conditions and compared the abundances of the species present with and without the new RR rate coefficients. We find that the new RR data have

no significant effects on the model results (i.e., less than a factor of 2 effect). We have also included DR for He^+ , C^+ , N^+ , O^+ , Na^+ , and Mg^+ in the 3 chemical models, finding some sizable differences (greater than a factor of 2) in the evolution of certain species.

We find that DR has the greatest effect for dense cloud models, particularly when surface chemistry is included. Of the models we ran here, only the OSU gas-grain code includes the extensive surface chemistry that allows species to be accreted onto grains and subsequently react with other surface species. Nahoon does not include this surface chemistry and the Meudon code only allows the formation of H_2 on surfaces. DR has its greatest influence for species that form on grain surfaces. These species may be particularly important in the warm-up phase of molecular clouds when they become desorbed into the gas phase. We find DR of C^+ to be primarily responsible for the abundance changes in the model. This is because charged species are assumed not to accrete onto grains and adding DR increases the gas-phase neutral C abundance available for first accreting onto grains and then participating in the surface chemistry.

We conclude by noting that there are some ions for which no state-of-the-art RR or DR data exist, specifically Si^+ , P^+ , S^+ , Cl^+ , and Fe^+ . Given the fine structure present in the ground terms of Si^+ , Cl^+ , P^+ , and Fe^+ one would expect a significant DR component to the total electron-ion recombination rate coefficient at low temperatures for these ions. These 4 elements also have first ionization potentials below that of H (13.6 eV). Given that they would thus be ionized in molecular clouds, the effect of increasing their recombination rates may be important. Modern calculations of both RR and DR rate coefficients for these ions are needed for generating reliable molecular cloud chemical models.

REFERENCES

- Aldrovandi, S. M. V., & Péquignot, D. 1973, *A&A*, 25, 137
- Arnaud, M., & Raymond, J. C. 1992, *ApJ*, 398, 394
- Badnell, N. R. 2006, *ApJS*, 167, 334
- Badnell, N. R., et al. 2003, *A&A*, 406, 1151
- Garrod, R. T., & Herbst, E. 2006, *A&A*, 457, 927
- Garrod, R. T., Wakelam, V., & Herbst, E. 2007, *A&A*, 467, 1103
- Gibb, E. L., Whittet, D. C. B., Boogert, A. C. A., & Tielens, A. G. G. M. 2004, *ApJS*, 151,

- Graedel, T. E., Langer, W. D., & Frerking, M. A. 1982, *ApJS*, 48, 321
- Hasegawa, T. I., Herbst, E., & Leung, C. M. 1992, *ApJS*, 82, 167
- Mazzotta P., Mazzitelli, G., Colfrancesco, S., & Vittorio, N. 1998, *A&AS*, 133, 403
- Nahar, S. N., & Pradhan, A. K. 1997, *ApJS*, 111, 339
- Nahar, S. N., & Pradhan, A. K. 1999, *ApJS*, 120, 131
- le Petit, F., Roueff, E., & le Bourlot, J. 2002, *A&A*, 390, 369
- le Petit, F., Nehmé, C., le Bourlot, J., & Roueff, E. 2006, *ApJS*, 164, 506
- Pety, J., Teyssier, D., Fossé, D., Gerin, M., Roueff, E., Abergel, A., Habart, E., & Cernicharo, J. 2005, *A&A*, 435, 885
- Roueff, E., le Bourlot, J., & Pineau Des Forêts, G. 1996, in *Dissociative Recombination: Theory, Experiment and Applications*, ed. D. Zajfman, J. B. A. Mitchell, D. Schwalm, B. R. Rowe (Singapore: World Scientific), 11
- Schull, J. M., & van Steenberg, M. 1982, *ApJS*, 48, 95 (erratum 49, 351)
- Smith, I. W. M., Herbst, E., & Chang, Q. 2004, *MNRAS*, 350, 323
- Vasyunin, A. I., Sobolev, A. M., Wiebe, D. S., & Semenov, D. A. 2004, *Astron. Lett.*, 30, 566
- Vasyunin, A. I., Semenov, D., Henning, Th., Wakelam, V., Herbst, E., & Sobolev, A. M. 2008, *ApJ*, 672, 629
- Verner, D. A., & Ferland, G. J. 1996, *ApJS*, 103, 467
- Wakelam, V., Caselli, P., Ceccarelli, C., Herbst, E., & Castets, A. 2004, *A&A*, 422, 159
- Wakelam, V., Selsis, F., Herbst, E., & Caselli, P. 2005, *A&A*, 883, 891
- Wakelam, V., Herbst, E., & Selsis, F. 2006, *A&A*, 451, 551
- Watson, W. D. 1976, *Rev. Mod. Phys.*, 48, 513
- Woodall, J., Agúndez, M., Markwick-Kemper, A. J., & Millar, T. J. 2007, *A&A*, 466, 1197

Table 1. Initial species abundances relative to the total H nuclei density, and physical conditions for dense clouds, protostars, and dense and diffuse PDRs.

Parameter	Initial conditions			
	Dense Cloud	Protostar ¹	Diffuse PDR	Dense PDR
H	–	–	9.90×10^{-1}	9.90×10^{-1}
He	1.40×10^{-1}	1.40×10^{-1}	1.00×10^{-1}	1.00×10^{-1}
N	2.14×10^{-5}	2.14×10^{-5}	7.50×10^{-5}	7.50×10^{-5}
O	1.76×10^{-4}	1.76×10^{-4}	3.19×10^{-4}	3.19×10^{-4}
F	6.68×10^{-9}	6.68×10^{-9}	–	–
C ⁺	7.30×10^{-5}	7.30×10^{-5}	1.32×10^{-4}	1.32×10^{-4}
Na ⁺	2.00×10^{-9}	2.00×10^{-9}	–	–
Si ⁺	8.00×10^{-9}	8.00×10^{-9}	–	–
S ⁺	8.00×10^{-8}	8.00×10^{-8}	1.86×10^{-5}	1.86×10^{-5}
Mg ⁺	7.00×10^{-9}	7.00×10^{-9}	–	–
P ⁺	3.00×10^{-9}	3.00×10^{-9}	–	–
Cl ⁺	4.00×10^{-9}	4.00×10^{-9}	–	–
Fe ⁺	3.00×10^{-9}	3.00×10^{-9}	1.50×10^{-8}	1.50×10^{-8}
H ₂ O	–	5.00×10^{-5}	–	–
H ₂ CO	–	2.00×10^{-6}	–	–
CH ₄ O	–	2.00×10^{-6}	–	–
CH ₄	–	5.00×10^{-7}	–	–
Temperature (K)	10	100	20	90
H ₂ density (cm ⁻³)	1×10^4	1×10^7	25	5×10^4
Cosmic ray ionization rate	1.3×10^{-17}	1.3×10^{-17}	5.0×10^{-17}	5.0×10^{-17}
Visual extinction	10	10	1	10

¹The elemental abundances are those at the beginning of the simulation, while the molecular abundances (H₂O, H₂CO, CH₄O, and CH₄) are set to the given values at a model time of 10⁵ years.

Note. — There is no F included in the OSU gas-grain code.

Table 2. Maximum abundance differences found when including DR in the OSU gas-grain code relative to excluding DR.

Species	Phase	Maximum Difference	Time (years)	Relative Abundance	Gas-Phase Detection ¹	Surface Detection ²
O ₃	Surface	1440	1.78×10^4	1.06×10^{-8}	No	No
N ₂ H ₂	Surface	59.3	3.16×10^4	1.47×10^{-12}	No	No
H ₂ O ₂	Surface	45.0	5.62×10^4	7.23×10^{-9}	No	No
HNCO	Gas	38.7	1.78×10^4	6.13×10^{-12}	Yes	No
HNCO	Surface	37.0	1.78×10^4	2.93×10^{-9}	Yes	No
NO	Surface	34.9	3.16×10^4	5.44×10^{-12}	Yes	No
NH ₂ CHO	Surface	30.0	5.62×10^4	3.46×10^{-11}	Yes	No
C ₂ H	Surface	27.2	1.00×10^4	1.06×10^{-12}	Yes	No
C ₂ H ₄	Surface	23.1	1.00×10^4	5.64×10^{-10}	Yes	No
HC ₂ O	Gas	18.3	1.78×10^4	2.41×10^{-12}	No	No
CH ₂ CO	Surface	15.0	1.00×10^4	3.10×10^{-10}	No	No
CH ₂ OH	Gas	14.1	1.00×10^4	5.47×10^{-12}	No	No
CH ₃ OH	Gas	13.8	1.00×10^4	3.26×10^{-12}	Yes	Yes
C ₃ H ₃ N	Surface	12.8	3.16×10^4	1.98×10^{-12}	No	No
HC ₃ N	Surface	12.5	3.16×10^4	3.77×10^{-11}	Yes	No
C ₂ H ₆	Gas	11.3	1.00×10^4	5.07×10^{-12}	No	No
CH ₂ NH ₂	Gas	9.76	5.62×10^4	1.96×10^{-12}	No	No
CH ₃ NH	Gas	9.76	5.62×10^4	3.65×10^{-12}	No	No
CH ₅ N	Surface	9.55	5.62×10^4	9.48×10^{-9}	No	No
C ₂ H ₂	Surface	8.27	1.00×10^4	1.19×10^{-9}	Yes	No
CH ₃ OH	Surface	7.59	3.16×10^4	2.43×10^{-8}	Yes	No
N ₂ H ₂	Gas	7.44	1.00×10^5	5.57×10^{-12}	No	No
CH ₃ CN	Surface	7.39	1.00×10^4	7.14×10^{-11}	Yes	No
HCN	Surface	7.37	1.78×10^4	1.24×10^{-8}	Yes	No
CH ₃	Surface	6.96	5.62×10^4	4.42×10^{-12}	Yes	No
CH ₂	Surface	6.96	5.62×10^4	4.46×10^{-12}	Yes	No
HNC	Surface	6.82	1.78×10^4	6.08×10^{-9}	Yes	No
CH	Surface	6.74	5.62×10^4	3.99×10^{-12}	Yes	Maybe
C	Surface	6.74	5.62×10^4	4.03×10^{-12}	No	No
C ₂ H ₆	Surface	6.63	3.16×10^4	1.25×10^{-8}	No	No

Table 2—Continued

Species	Phase	Maximum Difference	Time (years)	Relative Abundance	Gas-Phase Detection ¹	Surface Detection ²
N	Surface	6.51	5.62×10^4	1.99×10^{-12}	No	No
NH	Surface	6.51	5.62×10^4	2.02×10^{-12}	Yes	No
NH ₂	Surface	6.50	5.62×10^4	2.09×10^{-12}	Yes	No
O	Surface	6.40	5.62×10^4	1.48×10^{-11}	No	No
C ₄ H ₂	Surface	6.36	5.62×10^4	6.67×10^{-11}	Yes	No
C ₉ H ₂	Surface	6.35	5.62×10^4	1.00×10^{-12}	No	No
H ₂ CO	Surface	6.05	1.78×10^4	3.75×10^{-8}	Yes	Maybe
H ₂ C ₃ O	Gas	5.88	3.16×10^4	1.01×10^{-12}	Yes	No
HC ₃ O	Gas	5.88	3.16×10^4	1.90×10^{-12}	No	No
H ₂ C ₃ O	Surface	5.86	3.16×10^4	3.53×10^{-10}	Yes	No
C ₃ H ₂	Surface	5.70	5.62×10^4	1.50×10^{-8}	Yes	No
OH	Surface	5.49	5.62×10^4	1.24×10^{-11}	Yes	No
C ₅ H ₂	Surface	5.43	5.62×10^4	6.92×10^{-12}	No	No
CH ₂ NH	Gas	4.89	1.00×10^4	4.16×10^{-12}	Yes	No
O ₂	Surface	4.62	1.78×10^4	3.97×10^{-10}	Yes	No
O ₃	Gas	4.25	1.00×10^5	6.71×10^{-10}	No	No
H ₅ C ₃ N	Surface	3.75	3.16×10^4	1.03×10^{-10}	No	No
N ₂ O	Gas	3.48	1.00×10^4	5.05×10^{-11}	Yes	No
H ₂ S	Surface	3.41	5.62×10^4	5.08×10^{-9}	Yes	No
H ₂ O ₂	Gas	3.37	3.16×10^4	9.22×10^{-11}	No	No
CH ₅ N	Gas	3.26	1.00×10^4	2.19×10^{-12}	No	No
N ₂ O	Surface	3.19	1.78×10^4	1.40×10^{-12}	Yes	No
NO ₂	Gas	3.04	1.00×10^4	2.27×10^{-11}	No	No
HNO	Gas	2.98	1.00×10^4	2.97×10^{-10}	Yes	No
HNO	Surface	2.76	1.00×10^4	8.76×10^{-9}	Yes	No
CH ₃ CN	Gas	2.71	1.00×10^4	6.84×10^{-12}	Yes	No
C ₆ H ₂	Surface	2.69	3.16×10^4	1.17×10^{-12}	Yes	No
NO ₂	Surface	2.62	3.16×10^4	1.05×10^{-12}	No	No
C ₃ H	Surface	2.44	1.00×10^4	1.02×10^{-12}	Yes	No
CO ₂	Surface	2.23	1.00×10^4	2.08×10^{-10}	Yes	Yes

Table 2—Continued

Species	Phase	Maximum Difference	Time (years)	Relative Abundance	Gas-Phase Detection ¹	Surface Detection ²
CH ₃ CO ⁺	Gas	2.16	1.00×10^4	2.59×10^{-12}	No	No
HC ₂ NC	Gas	2.09	1.00×10^4	1.51×10^{-12}	Yes	No
C ₃ H ₃ ⁺	Gas	2.09	1.00×10^4	2.55×10^{-12}	No	No
HC ₃ N	Gas	2.02	1.00×10^4	2.99×10^{-11}	Yes	No
H ₂ CS	Surface	0.141	1.00×10^4	1.93×10^{-12}	Yes	No
C ₂ S	Surface	0.210	5.62×10^4	1.25×10^{-12}	Yes	No
C ₅ H ₄	Surface	0.292	1.00×10^4	2.82×10^{-12}	No	No
C ₃ H ₄	Surface	0.323	1.00×10^4	4.01×10^{-9}	No	No
CS	Surface	0.325	1.00×10^4	1.71×10^{-12}	Yes	No
C ₆ H ₄	Surface	0.349	1.78×10^4	4.65×10^{-13}	No	No
HS ₂	Gas	0.384	5.62×10^4	6.88×10^{-12}	No	No
H ₂ S ₂	Gas	0.386	5.62×10^4	6.99×10^{-12}	No	No
H ₂ S	Gas	0.392	3.16×10^4	1.80×10^{-10}	Yes	No
H ₃ S ⁺	Gas	0.413	5.62×10^4	7.64×10^{-13}	No	No

Note. — We list the maximum difference factor in abundance when DR is included in the OSU gas-grain code relative to when it is left out. At the relevant time in the model evolution, we list the abundance of each species relative to total H nuclei density when DR is included. We also list whether there has been an interstellar detection of the molecule in the gas phase or on dust surfaces.

¹http://astrochymist.org/astrochymist_ism.html

²Gibb et al. (2004)

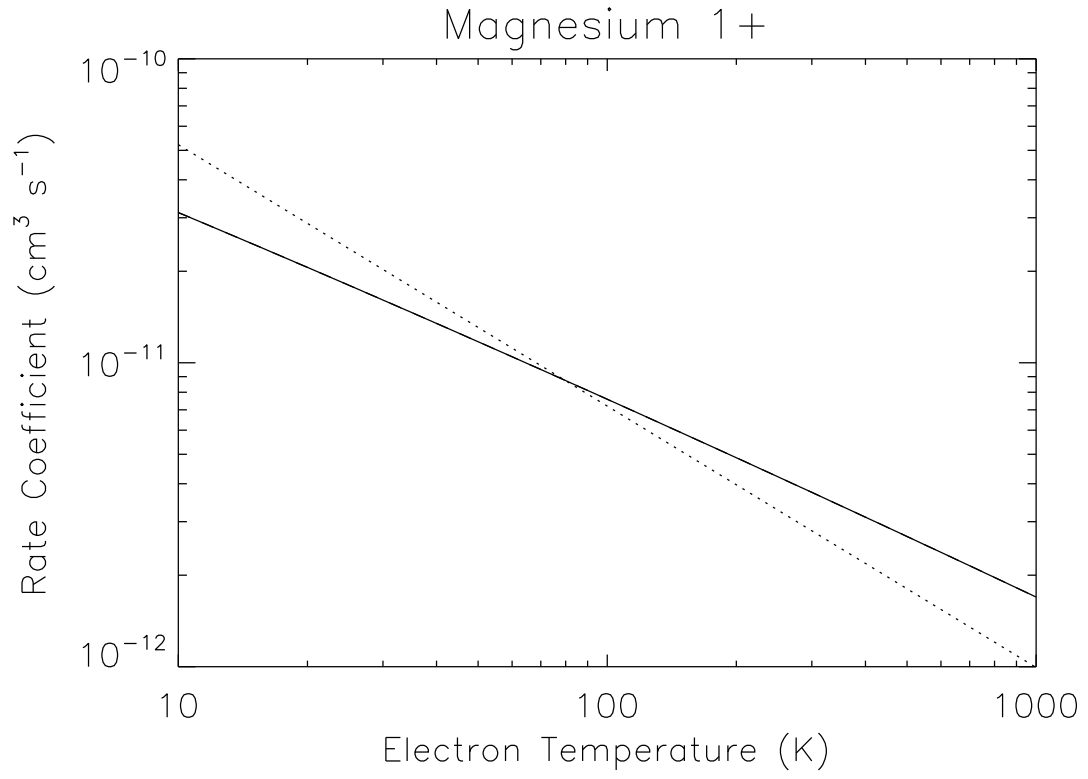


Fig. 1.— The RR rate coefficient for Mg^+ forming Mg. The dotted line is the rate coefficient from the UMIST database and the solid line shows the modern calculation of Badnell (2006).

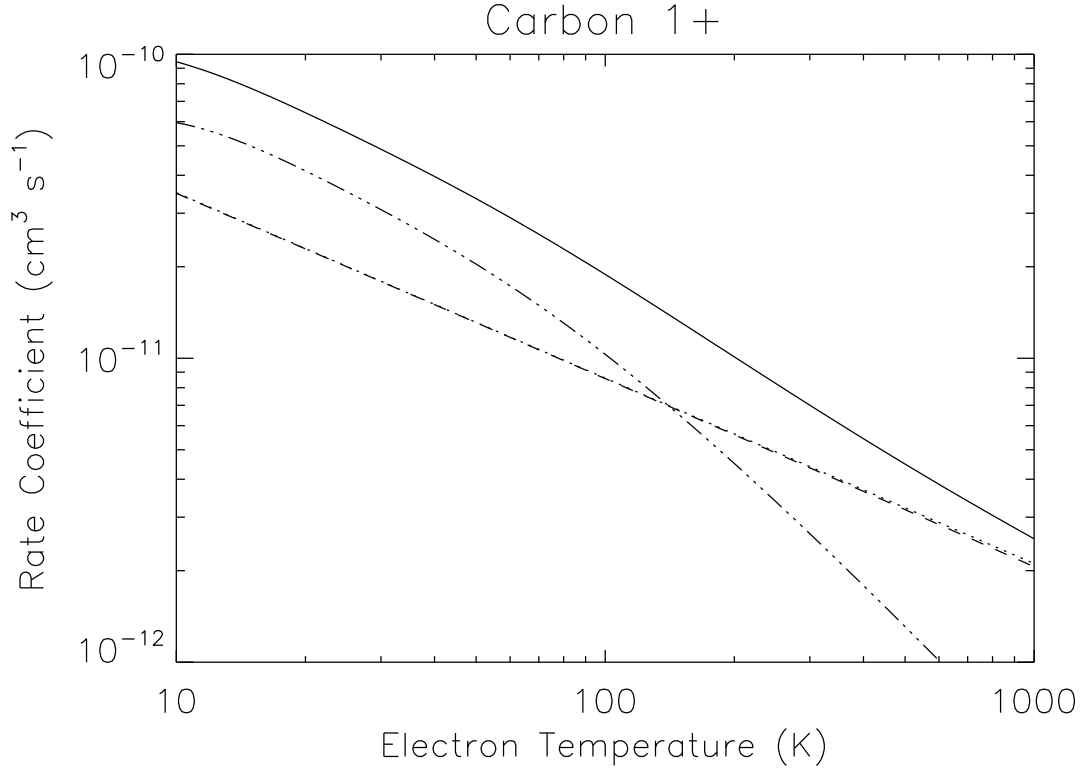


Fig. 2.— The DR and RR rate coefficients for C^+ forming C. The dotted line is the RR rate coefficient from the UMIST database. The dashed line shows the modern RR calculation of Badnell (2006) and lies almost exactly on top of the UMIST data. The dot-dot-dot-dashed line shows the DR calculation of Badnell et al. (2003). The solid line is the total RR+DR recombination rate coefficient of Badnell.

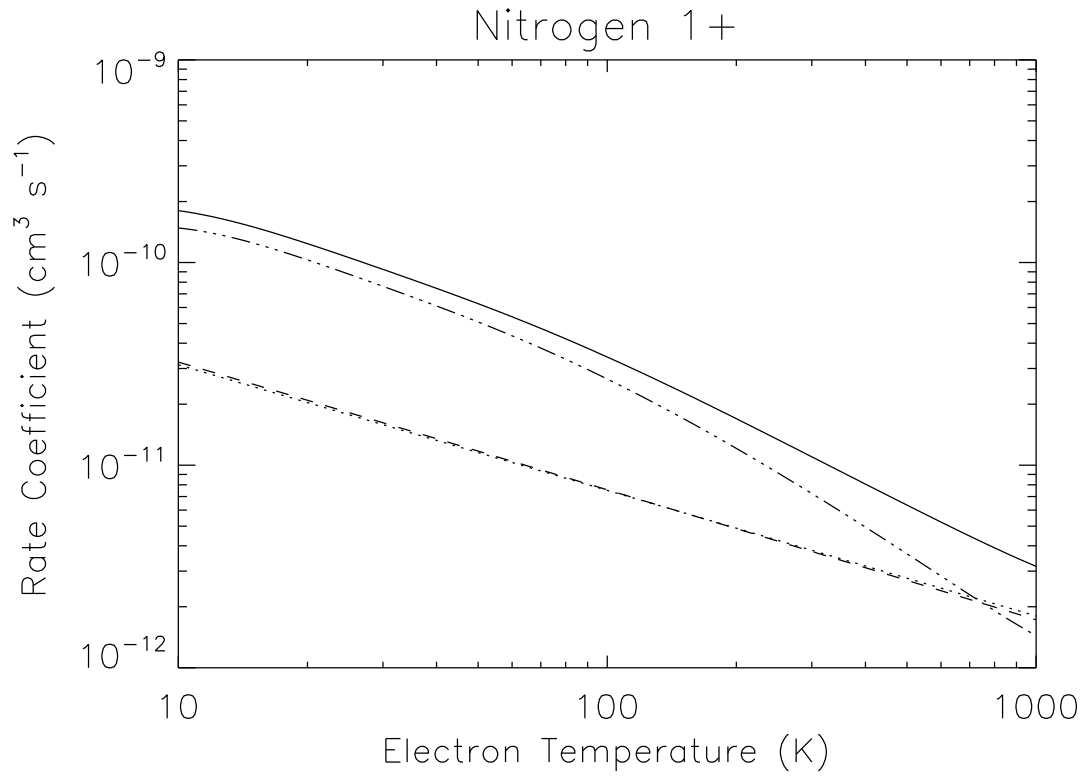


Fig. 3.— Same as Fig. 2 but for N^+ forming N.

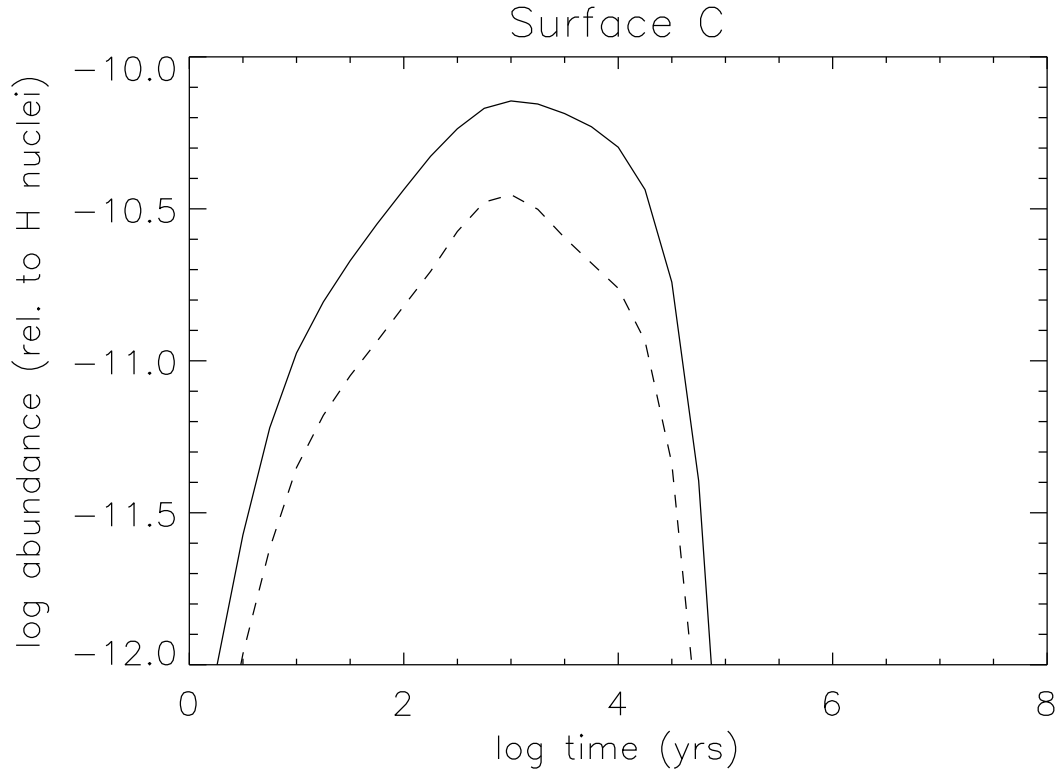


Fig. 4.— The abundance of surface C with respect to the total H nuclei density as a function of time as calculated by the OSU gas-grain code. The solid line is with the new RR and DR data included in the model and the dotted line is without the new RR and DR included.

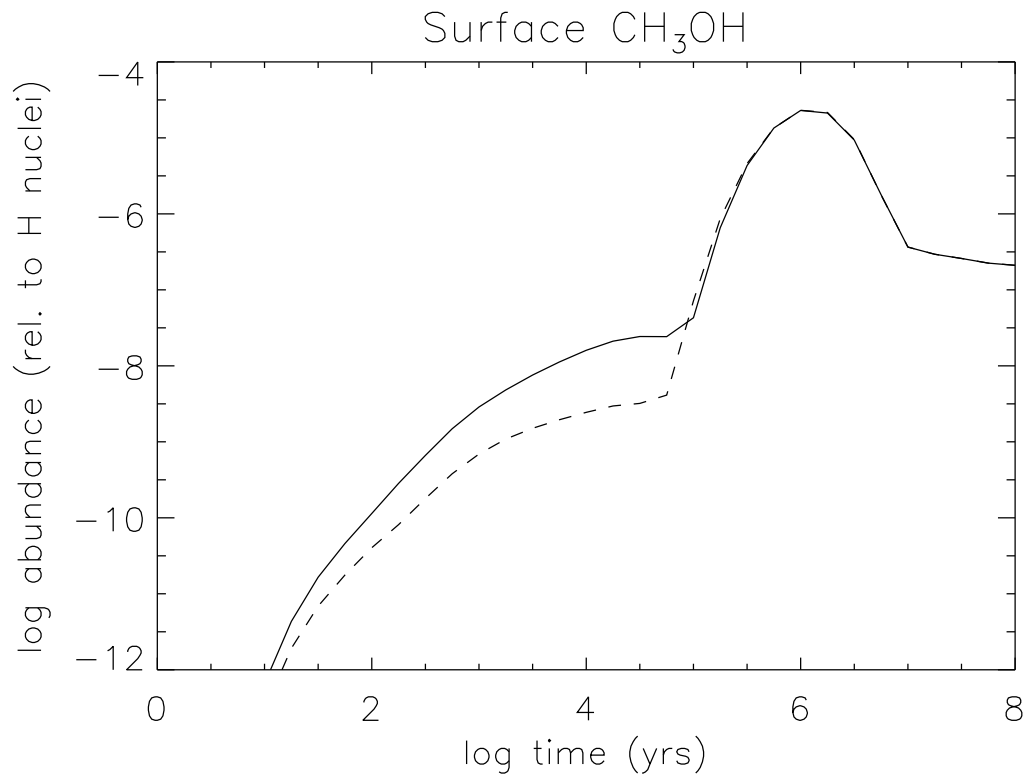


Fig. 5.— Same as Fig. 4 but for surface CH_3OH .

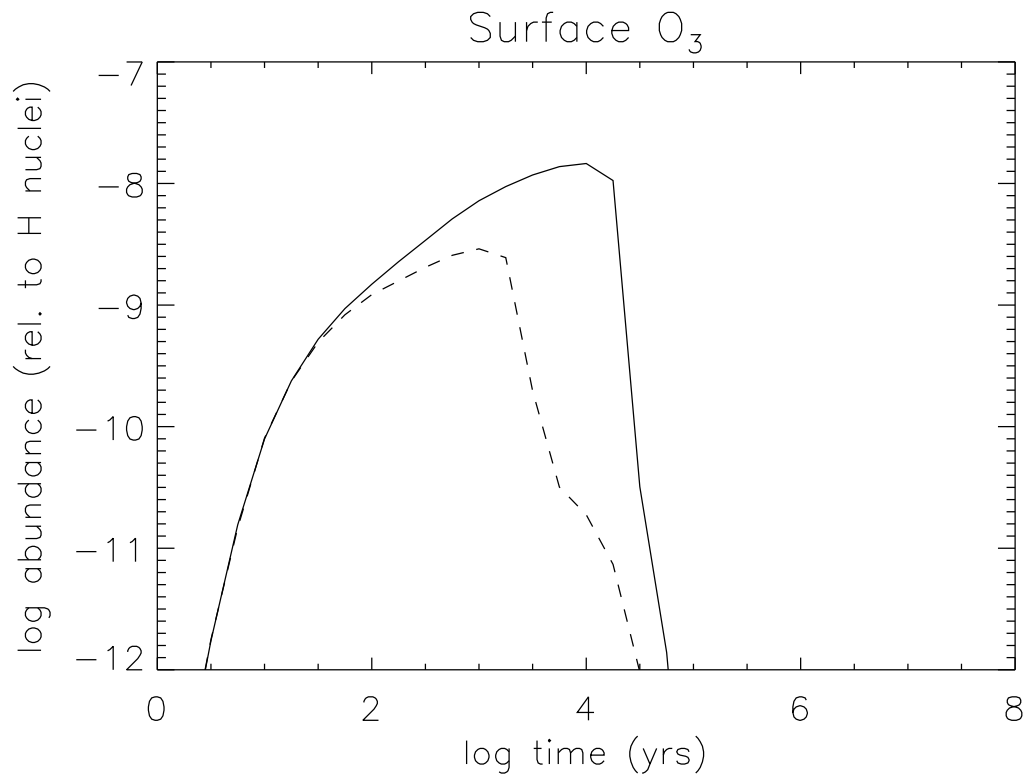


Fig. 6.— Same as Fig. 4 but for surface O_3 .

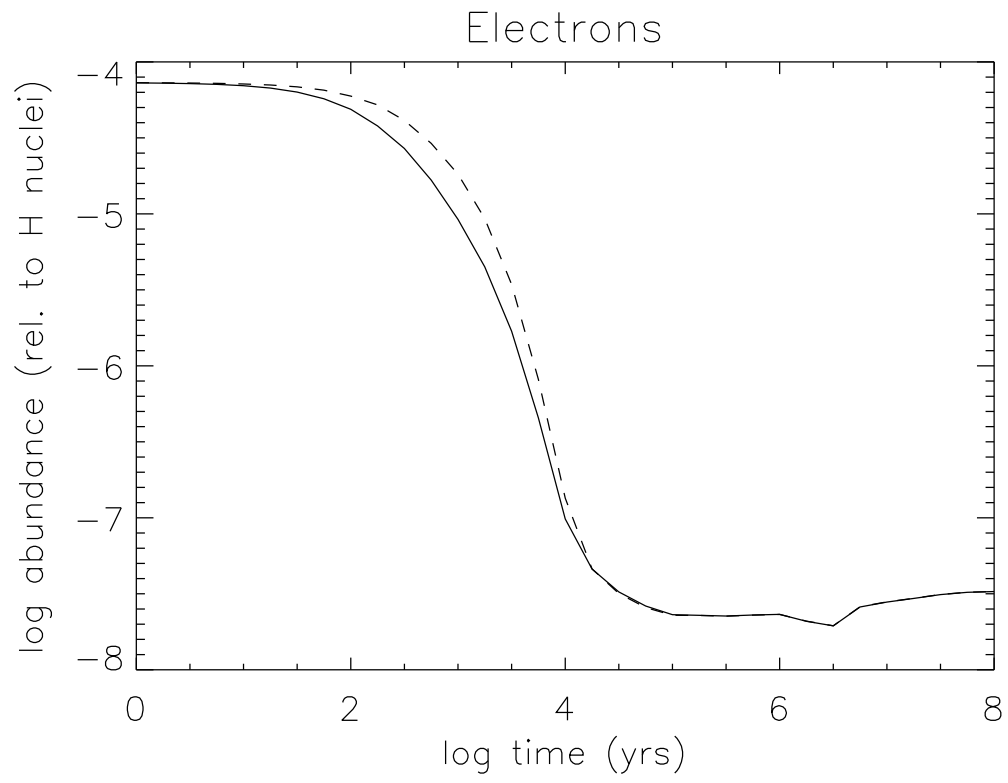


Fig. 7.— Same as Fig. 4 but for free electrons.

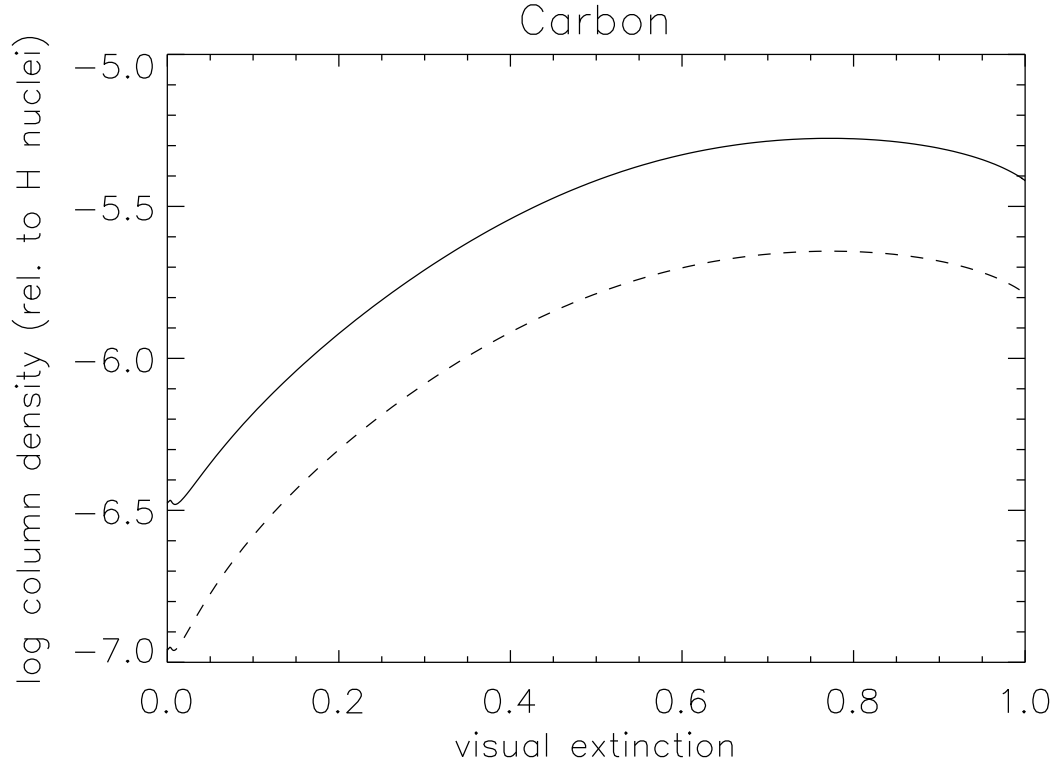


Fig. 8.— The column density of C relative to the total H nuclei column density as a function of visual extinction (i.e., depth into the cloud) calculated by the Meudon PDR code for a diffuse PDR. The solid line is with the new RR and DR included in the model and the dashed line is without the new RR and DR included.

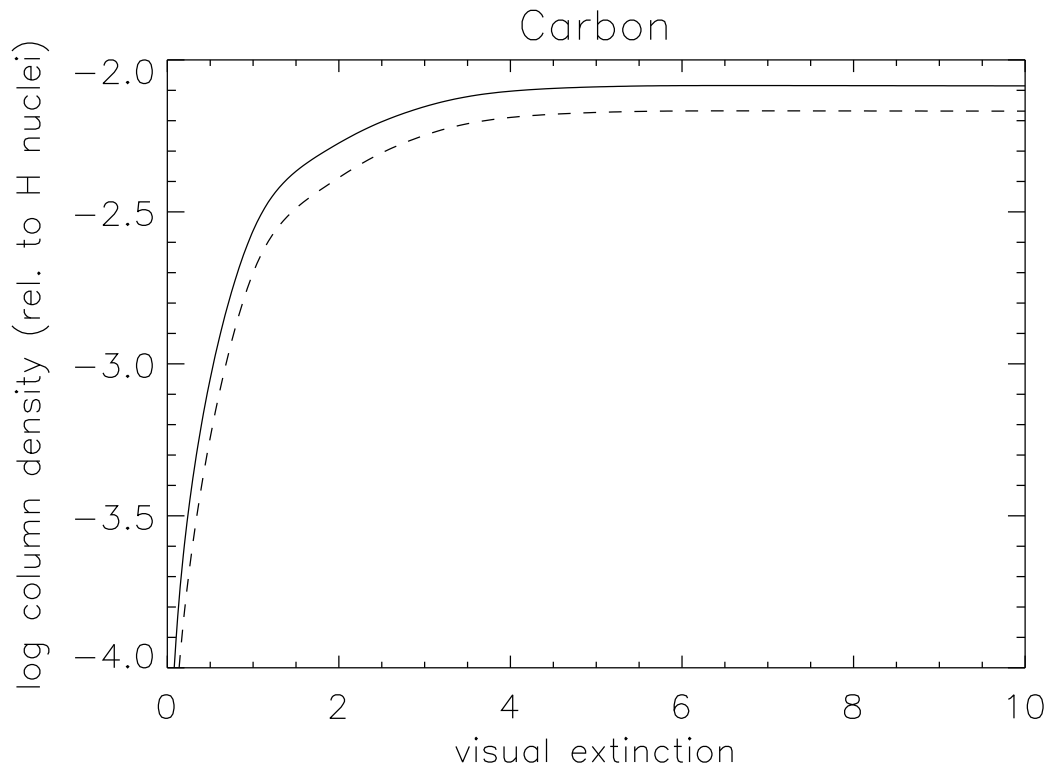


Fig. 9.— Same as Fig. 8 but for a dense PDR.